Water/n-alkane mixtures: Modelling with SAFT-VR-SW and SAFT-γ-Mie GC approach

Rita Patrício Gomes
Universidade Técnica de Lisboa, 1049-001 Lisboa, Portugal

Abstract: The water/n-alkane mixtures are very important for the reality we live in, where the most used source of energy is petroleum. Given the importance of predicting the thermodynamic properties of this type of systems, two approaches of the Statistical Associating Fluid Theory (SAFT) were used to predict the mutual solubility, and the thermodynamic functions of the water/n-hexane, water/n-heptane, water/n-undecane and water/n-hexadecane system. The SAFT-VR-SW theory was used, where molecules are modeled as chains of spherical segments with attractive forces represented with the square-well potential. In this approach a binary interaction parameter, K_{ij}, was fitted for each system, in the oil rich phase. The solubility curves obtained where a much better prediction of the experimental data than those obtained with no fitted K_{ij}. The SAFT-γ-Mie approach was also used to describe the water/n-alkane systems. SAFT-γ-Mie is formulated within the framework of a group contribution approach, where molecules are represented as chains of heteronuclear fused spheres comprising distinct functional chemical groups, where interaction between segments are described with the Mie potential of variable attractive and repulsive range. This approach presented the best results in the prediction of the mutual solubility of the studied systems. With the solubility results of the oil-rich phase obtained with both theories, the thermodynamic functions of solution, $\Delta_{sol}H_m^0$, $\Delta_{sol}S_m^0$, and solvation, $\Delta_{svt}H_m^0$ and $\Delta_{svt}S_m^0$were also obtained. The results showed that the thermodynamic functions obtained from the predictions of both theories, SAFT-VR-SW and SAFT-γ-Mie are able to describe the experimental results, although these presented a more pronounced dependence with the chain length of the alkane.

Introduction

It's of common knowledge that the world we live in needs an incredible amount of energy. Despite the efforts devoted to renewable and ecologically friendly sources of energy, petroleum continues to be the most important one. The operational costs of the extraction, transport, and transformation are increasing while the source amount is thought to be decreasing, (Ferguson, Debenedetti, & Panagiotopoulos, 2009). Therefore, is necessary to optimize the process through a better knowledge of the thermodynamic behavior of petroleum, which is, chemically, a complex mixture of hydrocarbons. Given the need for a considerably quantity of data in a large spectrum of temperatures and pressure and in order to permit the optimization of the processes, it's necessary to find more accurate models to describe the mutual solubility and thermodynamic properties between these compounds.

Mixtures of water and hydrocarbons exhibit limited miscibility over a wide range of temperatures, thus giving rise to two distinct phases: A hydrocarbon - rich phase containing a very small concentration of water molecules and a water-rich phase, containing an even smaller concentration of dissolved hydrocarbon. Water-hydrocarbons mixtures are very non-ideal mixtures, since water and hydrocarbons are very different substances, engaging in different interactions with one another. For instance, between hydrocarbons, dispersive interactions prevail, while in the water rich phase, since water is a small polar molecule, capable of establishing strong hydrogen bonds, this type of interaction prevails.

When a hydrocarbon molecule is dissolved in water, a number of hydrogen bonds are broken depending on the size of the cavity needed to accommodate the hydrocarbon molecule, therefore, on the size and shape of

the hydrocarbon. The water molecules around the hydrocarbon rearrange in order to maximize the formation of hydrogen bonds, this is known as hydrophobic effect. From this effect results a decrease of entropy since water molecules rearrange in order to be able to establish new hydrogen bonds, resulting in a more organized arrangement.

On the hydrocarbon rich phase, when water is dissolved, the situation is very different. Considering that first one has pure water and pure n-alkane, when water is added to the n-alkane in a very small proportion of water molecules/alkane molecules, all of the hydrogen bonds of the pure water are broken, and water molecules are isolated between n-alkane molecules. The solubility of water in different hydrocarbons is not identical because hydrocarbons, depending on their polarizability, engage in weak but variable van der Waals interactions with water (Wisniewska-Goclowska, Shaw, Skrzecz, Góral, & Maczynski, 2003).

Despite the technological importance of accurate data on mutual alkane-water solubilities, the available literature values are widely scattered and it is not easy to decide on a coherent set of data to use as reference.

The purpose of this work is the study and modeling of four binary water/alkane systems, water/n-hexane, water/n-heptane, water/n-undecane and water/n-hexadecane, using two different versions of the SAFT EoS. New unpublished solubility data of water in the n-alkanes obtained in our research group's was used. The SAFT-VR-SW and the SAFT-γ-mie versions of the theory were used to describe the mutual solubility of these specific water/n-alkane systems, but the study mainly focused on the alkane rich phase.The thermodynamic functions of solution and solvation of water in the alkane rich phase, $\Delta_{sol}H_m^0$, $\Delta_{sol}S_m^0$, $\Delta_{svt}H_m^0$ and $\Delta_{svt}S_m^0$, were calculated for each system. The main goal of the analysis is to allow a better understanding of the water/n-alkanes interactions on the oil rich phase and in particular its dependence with the n-alkanes chain length.

State of the art

The importance of equations of state in Chemical Engineering can hardly be overestimated. The development of accurate molecular equations of state for the thermodynamic properties of fluids of associating molecules, is an important goal as it provides a framework for the representation of the behavior of real fluids and their mixtures with minimal computational cost.(Galindo & Mccabe, 2010).

One of the major advances in the theoretical modelling of complex fluids comes from the work of Wertheim (Wertheim, 1984) back in the 1980's, on associating and polymeric fluids and its implementation as an equation of state (EoS) by Champman, Gubbins, Radosz, and Jackson as the statistical associating fluid theory (SAFT), (Chapman, Gubbins, Jackson, & Radosz, 1989). Numerous versions of the SAFT EoS can be found today of which soft-SAFT (Blas & Vega, 1997), SAFT-VR (Gil-Villegas, et al., 1997), PC-SAFT (Gross & Sadowski, 2001) and SAFT-γ–Mie (Lafitte, et al., 2013) are, perhaps, the main examples.

In the statistical associating fluid theory, (Chapman, Gubbins,, Jackson, & Radosz, 1989), molecules are modelled as associating chains formed of bonded spherical segments, with short ranged attractive sites, used as appropriate to mediate association interactions. The Helmholtz energy is written as the sum of four separate contributions:

$$\frac{\mathrm{A}}{\mathrm{Nk_B T}} = \frac{\mathrm{A_{Ideal}}}{\mathrm{Nk_B T}} + \frac{\mathrm{A_{Mono}}}{\mathrm{Nk_B T}} + \frac{\mathrm{A_{Chain}}}{\mathrm{Nk_B T}} + \frac{\mathrm{A_{Assoc.}}}{\mathrm{Nk_B T}} \qquad (1)$$

Where A_{Ideal} is the ideal free energy, $A_{Mono.}$ the contribution to the free energy due to the monomer-monomer repulsion and dispersion interactions, A_{Chain} the contribution due to the formation of bonds between monomeric segments, and $A_{Assoc.}$ the contribution due to association.

There are numerous studies in the literature focusing on the application of different versions of the SAFT EoS to describe the water/alkane systems. In the work of (Patel, Galindo, Maitland, & Paricaud, 2003) the salting out of *n*-alkanes in water by strong electrolytes using an extension of the statistical associating fluid theory for attractive potentials of variable range, which incorporates ionic interactions, is investigated. The phase behavior of the binary water + *n*-alkane mixtures is well described by the theoretical approach using two unlike

adjustable parameters which are transferable for different alkane molecules.

(Vega, Llovell, & Blas, 2009) published a study where they were able to capture the solubility minima of *n*-alkanes in water using soft-SAFT. The purpose of their work was to find a molecular model for water, within the soft-SAFT framework, capable of describing the water/n-alkanes mixtures at room temperature. The equation was able to predict the mutual solubilities, with a single transferable energy binary parameter,ξ, independent of temperature and chain length.

SAFT-VR-SW

In the present work the SAFT-VR-SW was used to obtain solubility data of different water/n-alkanes systems.

Intermolecular potential

The considered hard-core potential used in this work is the square-well in which both repulsive and attractive interactions are included. It can be defined as,

$$\mathrm{u^{SW}(r)} = \begin{cases} \infty \; if \; r < \sigma \\ -\epsilon \; \mathrm{if} \; \sigma \le \mathrm{r} \le \lambda\sigma \\ 0 \; \mathrm{if} \; \mathrm{r} > \lambda\sigma \end{cases} \qquad (2)$$

where *r* is the intermolecular centre-to-centre distance, σ the hardcore diameter, ϵ the depth of the attractive well and λ its range. In the square well, the energy is constant over the range of interaction.

Ideal term

The free energy of an ideal gas is given as by,

$$\frac{\mathrm{A^{ideal}}}{\mathrm{Nk_BT}} = (\sum_{i=1}^{n} x_i \ln(\rho_\mathrm{i}\Lambda_\mathrm{i}^3))\text{-}1 \qquad (3)$$

Where $x_i = {N_i}/{N}$ is the mole fraction, $\rho_i = {N_i}/{V}$ is the molecular number density, N_i is the number of molecules, Λ_i is the thermal de Broglie wavelength of species *i,* and *V* is the volume of the system.

Monomer term

The monomers contribution to the Helmholtz free energy (m of which make up each chain) is given by the following expression,

$$\frac{\mathrm{A^{mono.}}}{\mathrm{Nk_BT}} = \left(\sum_{i=1} x_i m_i\right)\frac{\mathrm{A^M}}{\mathrm{N_s k_B T}} = \left(\sum_{i=1} x_i m_i\right)\mathrm{a^M} \qquad (4)$$

For which m_i is the number of spherical segments of chain *i*, N_s is the total number of spherical monomers, and $a^M$is the excess Helmholtz free energy per monomer.

Chain term

The contribution to the free energy due to the formation of a chain of *m* monomers is,

$$\frac{\mathrm{A^{chain}}}{\mathrm{Nk_BT}} = -\left(\sum_{i=1}^{n} x_i(m_i - 1)\right)\ln y_{ii}^{SW}(\sigma_{ii}) \qquad (5)$$

Association Term

The contribution due to association for *s* sites on chain molecules is obtained from,

$$\frac{\mathrm{A^{Assoc.}}}{\mathrm{Nk_BT}} = \left[\sum_{\mathrm{a}=1}^{\mathrm{s}}\left(\ln \mathrm{X_a} - \frac{\mathrm{X_a}}{2}\right) + \frac{\mathrm{s}}{2}\right] \qquad (6)$$

taking in account that the sum is over all *s* sites *a* on a molecule, and that X_a is the fraction of molecules not bonded at site *a,* X_a is then obtained by a solution of the following mass action equation.

Water model

In this work the chosen model is the four-site water model. In this model the two hydrogen bonding interactions are mediated through off-center square-well bonding sites of types *H* (Hydrogen) and *e* (electron lone pairs), located halfway between the center and the surface of the molecular core. Only *e-H* bonding is considered, and multiple bonding at a given site is forbidden. When an *e* and an *H* site come within a cut-off range $r_{c;H,e}$ of each other there is a site-site hydrogen-bonding associative interaction.

Combining rules

In the SAFT-VR approach the used combining rules are presented in the following expressions, (McCabe C. , Galindo, Gil-Villegas, & Jackson, 1998).

The unlike size is calculated using the Lorentz rule,

$$\sigma_{ij} = \frac{\sigma_{ii} + \sigma_{jj}}{2} \qquad (7)$$

Where the energy parameters are calculated recurring to the following equation,

$$\epsilon_{ij} = (1 - k_{ij})\sqrt{\epsilon_{ii}\epsilon_{jj}} \qquad (8)$$

The unlike range parameter is through the following equation,

$$\lambda_{ij} = (1 - \gamma_{ij})\frac{\lambda_{ii}\sigma_{ii} + \lambda_{jj}\sigma_{jj}}{\sigma_{ii} + \sigma_{jj}} \qquad (9)$$

Results and discussion

The parameters characterizing the chosen water model were optimized to vapor–liquid equilibria data and are reported in table 1, (Clark G. N., Haslam, Galindo, & Jackson, 2006). The parameters λ, σ and ϵ /k used were those reported by (Paricaud, Jackson, & Galindo, 2004) obtained optimizing the description of the experimental vapor pressure and density for the various alkanes, and are reported in table 2.

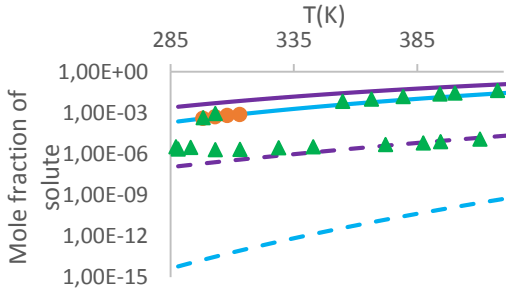

Figure 1- Mole fraction of water in n-hexane (solid line) and of n-hexane in water (dotted line); experimental data (Maczynski A. , Shaw, Goral, & Wisniewska-Goclowska, 2005) (triangles); experimental data (Morgado, 2011) (circles); prediction from SAFT-VR-SW with k_{ij}=0 (purple) and SAFT-VR-SW results k_{ij}=0,30 (blue).

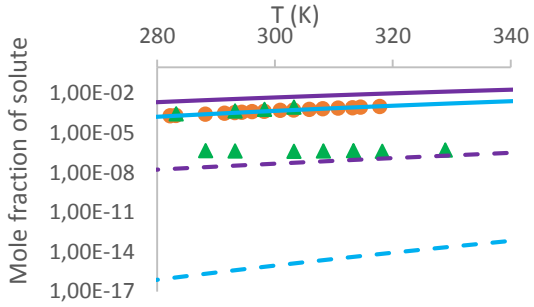

Figure 2- Mole fraction of water in n-heptane (solid line) and of n-heptane in water (dotted line); experimental data (Maczynski A. , Shaw, Goral, & Wisniewska-Goclowska, 2005) (triangles); experimental data (Morgado, 2011) (circles); prediction from SAFT-VR-SW with k_{ij}=0 (purple) and SAFT-VR-SW results k_{ij}=0,29 (blue).

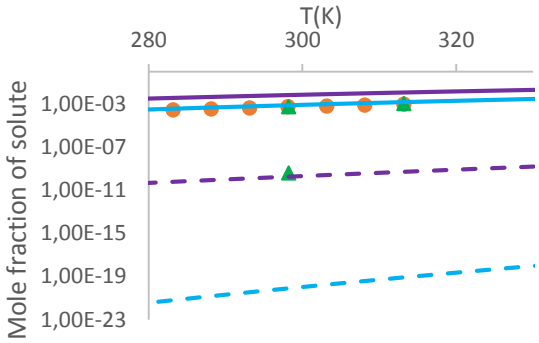

Figure 3- Mole fraction of water in n-undecane (solid line) and of n-undecane in water (dotted line); experimental data (Maczynski A. , Shaw, Goral, & Wisniewska-Goclowska, 2005) (triangles); experimental data (Morgado, 2011) (circles); prediction from SAFT-VR-SW with k_{ij}=0 (purple) and SAFT-VR-SW results k_{ij}=0,26 (blue).

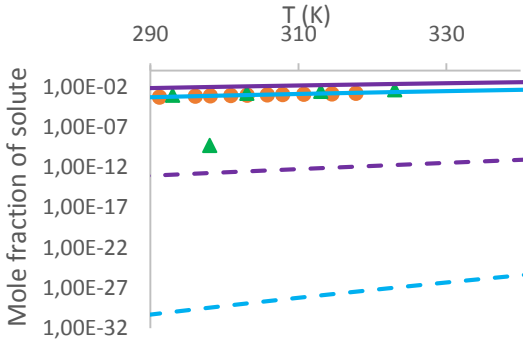

Figure 4- Mole fraction of water in n-hexadecane (solid line) and of n-hexadecane in water (dotted line); experimental data (Maczynski A. , Shaw, Goral, & Wisniewska-Goclowska, 2005) (triangles); experimental

data (Morgado, 2011) (circles); prediction from SAFT-VR-SW with k_{ij}=0 (purple) and SAFT-VR-SW results k_{ij}=0,30 (blue).

As can be observed, in all systems the theoretical predictions with k_{ij}=0 overpredict the experimental solubility of water in the hydrocarbon-rich phase (solid line). For the water-rich phase (square dot line), in the case of water/n-heptane, n-undecane and n-hexadecane, the theoretical results underpredict the experimental solubility, although in the case of water/n-undecane the prediction is very close to the experimental value. In the case of water/n-hexane, however, the theoretical results are in good agreement with the experimental results at the higher temperatures (higher than 340K), but underpredict at lower temperatures. It is also important to note that the shape of the curve in the water rich phase does not follow the trend of the experimental results.

Analyzing the results for which the k_{ij} was fitted to the (Morgado, 2011) experimental data, one can see that for all systems the prediction for the oil rich phase is very good, better than in the previous case (k_{ij}=0). However, the predicted solubility of the n-alkanes in the water rich phase is largely underpredicted. These results demonstrate that optimizing the k_{ij} values to reproduce the experimental solubility of water in the n-alkanes lowers both sides of the system's curves resulting in a very good prediction on the oil rich phase but in much worse results on the water rich phase.

Table 1- m, λ, σ (Å) and ϵ /k used for the water model of SAFT-VR-SW (Clark G. N., Haslam, Galindo, & Jackson, 2006)

Compound	λ	σ (Å)	ϵ /k (K)	ϵ^{HB} /k (K)	r_c^{HB}(Å)	K^{HB}(Å^3)
Water	1,7889	3,0342	250	1400,00	2,1082	1,0667

Table 2 m, λ, σ (Å) and ε/k used for each studied compound using SAFT-VR-SW taken from (Paricaud, Jackson, & Galindo, 2004)

Compound	m	λ	σ (Å)	ϵ/k (K)
n-hexane	2,6667	1,5492	3,9396	251,66
n-heptane	3,0000	1,5574	3,9567	253,28
n-undecane	4,3333	1,5854	3,9775	252,65
n-hexadecane	6,0000	1,6325	3,9810	237,33

SAFT-γ-Mie GC approach

In the SAFT-γ-Mie GC approach, molecules are represented as comprising distinct functional chemical groups based on a fused heteronuclear molecular model, where the interactions between segments are described with the Mie potential of variable attractive and repulsive range.

The main aspects of the SAFT-γ-Mie Group contribution are presented, being the reader referred to the original papers for deeper insight (Papaioannou, et al., 2014).

Intermolecular Potential

Each chemical functional group *k* is represented as a fused spherical segment or number of segments v_k^*. Two segments *k* and *l* are assumed to interact via a Mie potential of variable range:

$$\Phi_{kl}^{Mie}(r_{kl}) = C_{kl}\epsilon_{kl}\left[\left(\frac{\sigma_{kl}}{r_{kl}}\right)^{\lambda_{kl}^{r}} - \left(\frac{\sigma_{kl}}{r_{kl}}\right)^{\lambda_{kl}^{a}}\right] \qquad (10)$$

where $r_{kl}$is the distance between the centres of the segments, σ_{kl} the segment diameter, ϵ_{kl}

the depth of the potential well, and λ_{kl}^{r} and λ_{kl}^{a} the repulsive and attractive exponents of the segment-segment interactions, respectively. The prefactor C_{kl} is a function of these exponents and ensures that the minimum of the interaction is -ϵ_{kl}.

The Helmholtz free energy of this model can be obtained from the appropriate contributions of the different groups, noting that the implementation of this type of united-atom model of fused segments requires the additional use of a shape factor S_k, which reflects the proportion in which a given segment contributes to the total free energy. As in other SAFT approaches, hydrogen bonding or strongly polar interactions can be treated through the incorporation of a number of additional short-range square-well association sites, which are placed on any given segments as required. The association interaction between two square-well association sites of type *a* in segment *k* and *b* in segment *l* is given by,

$$\Phi_{kl,ab}^{HB}(r_{kl,ab}) = \begin{cases} -\epsilon_{kl,ab}^{HB} \text{ if } r_{kl,ab} \le r_{kl,ab}^{c}, \\ 0 \text{ if } r_{kl,ab} > r_{kl,ab}^{c}, \end{cases} \quad (11)$$

where $r_{kl,ab}$ is the center-center distance between sites *a* and *b*, $-\epsilon_{kl,ab}^{HB}$ is the association energy, and $r_{kl,ab}^{c}$ the cut-off range of the interaction between sites *a* and *b* on groups *k* and *l*, respectively. Each site is positioned at a distance $r_{kk,aa}^{d}$from the center of the segment on which it is placed.

The ideal term

The free energy corresponding to an ideal mixture of molecules is given by the following expression,

$$\frac{A^{ideal}}{Nk_BT} = \left(\sum_{i=1}^{N_C} x_i \ln(\rho_i \Lambda_i^3) - 1 \right) \quad (12)$$

where x_i is the mole fraction of component *i* in the fraction, $\rho_i = \frac{N_i}{V}$ the number density of component *i*, being N_i the number of molecules of component *i* and *V* the total volume of the system, *N* the total number of molecules, k_B the Boltzmann constant, and *T* the absolute temperature. The summation is over all of the components N_C of the mixture.

The monomer term

The free-energy contribution due to repulsion and attraction interactions for the monomeric fluid characterized by the Mie potential is obtained following a Barker-Henderson high temperature perturbation expansion up to third order, which can be expressed as

$$\frac{A^{mono.}}{Nk_BT} = \frac{A^{HS}}{Nk_BT} + \frac{A_1}{Nk_BT} + \frac{A_2}{Nk_BT} + \frac{A_3}{Nk_BT} \quad (13)$$

where the repulsive term A^{HS} is the free energy of a hard-sphere reference system of diameter d_{kk}, dependent of the temperature.

Chain term

In the SAFT-γ approach the change in free energy associated with the formation of a molecule from its constituting segments is obtained recurring to the average molecular parameters ($\overline{\sigma_{ii}}$, $\overline{d_{ii}}$, $\overline{\epsilon_{ii}}$ and $\overline{\lambda_{ii}}$), for each molecular species *i*. The resulting contribution to the free energy of the mixture due to the formation of chains of tangent (or fused) segments using the effective molecular parameters is given by

$$\frac{A^{chain}}{Nk_BT} = -\sum_{i=1}^{N_C} x_i \left(\sum_{k=1}^{N_G} v_{k,i} v_k^* S_k - 1 \right) \ln g_{ii}^{Mie}(\overline{\sigma_{ii}}, \zeta_x) \quad (14)$$

where $g_{ii}^{Mie}(\overline{\sigma_{ii}}, \zeta_x)$ is the value of the radial distribution function (RDF) evaluated at a distance $\overline{\sigma_{ii}}$ in a hypothetical fluid of packing fraction ζ_x.

Association Term

The Helmholtz free energy due to the association of molecules via short range bonding sites is obtained by summing over the number of species N_C, the number of groups N_G, and the number of site types on each group $N_{ST,k}$, as showed in the following equation,

$$\frac{A^{assoc.}}{Nk_BT} = \sum_{i=1}^{N_C} x_i \sum_{k=1}^{N_G} v_{k,i} \sum_{a=1}^{N_{ST,k}} n_{k,a} \left(\ln X_{i,k,a} + \frac{1 - X_{i,k,a}}{2} \right) \quad (15)$$

where $n_{k,a}$is the number of sites of type *a* on group *k*, and $X_{i,k,a}$is the fraction of molecules

of component *i*, that are not bonded at a site of type *a* on a group *k*.

Water Model

Group contribution techniques are generally not well suited for the study of small molecules as proximity effects are neglected, to have a more accurate model the water molecule is described as a separate functional group, capable only of associating between sites *H* and *e*. This water model is described by the parameters in tables 3,4 and 5.

Combining Rules

The study of binary and multicomponent systems requires a number of combining rules for the unlike intermolecular parameters. These are, determined using combining rules, and refined by estimation from experimental data when required.

The unlike segment diameter is obtained from a simple arithmetic mean,

$$\sigma_{kl} = \frac{\sigma_{kk}+\sigma_{ll}}{2} \qquad (16)$$

For the calculation of the unlike effective hard-sphere diameter, the same combining rule is applied,

$$d_{kl} = \frac{d_{kk}+d_{ll}}{2} \qquad (17)$$

As for the unlike dispersion energy, ϵ_{kl}, the system's mixture data is used since no pure molecule contains the interaction water -CH2 or water –CH3.

The combining rule for the repulsive, ${\lambda_{kl}}^{r}$, and the attractive, ${\lambda_{kl}}^{a}$, is given by equation 18.

$$\lambda_{kl} = 3 + \sqrt{(\lambda_{kk}-3)(\lambda_{ll}-3)} \qquad (18)$$

The unlike value of the association energy can be obtained by,

$${\epsilon_{kl}}^{HB} = \sqrt{{\epsilon_{kk,aa}}^{HB}{\epsilon_{ll,bb}}^{HB}} \qquad (19)$$

The unlike bonding volume $K_{kl,ab}$ is obtained as,

$$K_{kl,ab} = \left(\frac{\sqrt[3]{K_{kk,aa}}+\sqrt[3]{K_{ll,bb}}}{2}\right)^{3} \qquad (20)$$

Results ad discussion

The results obtained using the SAFT-γ-Mie theory are presented in figures 6 to 9.The results were obtained recurring to the HELD algorithm, used to calculate the equilibrium phases.

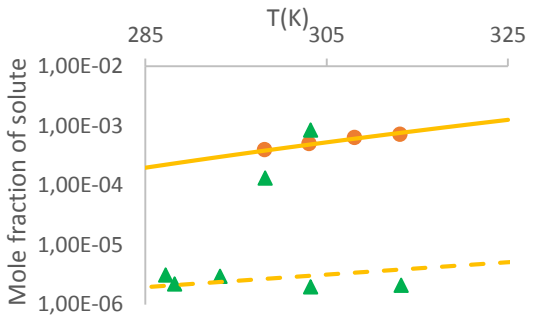

Figure 5- Mole fraction of water in n-hexane (solid line) and of n-hexane in water (dotted line) as a function of temperature; experimental data from (Maczynski A. , Shaw, Goral, & Wisniewska-Goclowska, 2005)(triangles); experimental data from (Morgado, 2011) (circles); SAFT- γ-Mie results (yellow line).

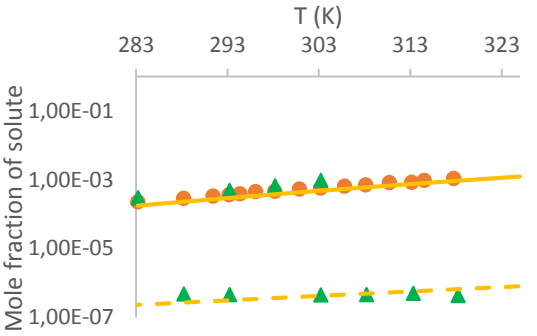

Figure 6- Mole fraction of water in n-heptane (solid line) and of n-heptane in water (dotted line) as a function of temperature; experimental data from (Maczynski A. , Shaw, Goral, & Wisniewska-Goclowska, 2005)(triangles); experimental data from (Morgado, 2011) (circles); SAFT- γ-Mie results (yellow line).

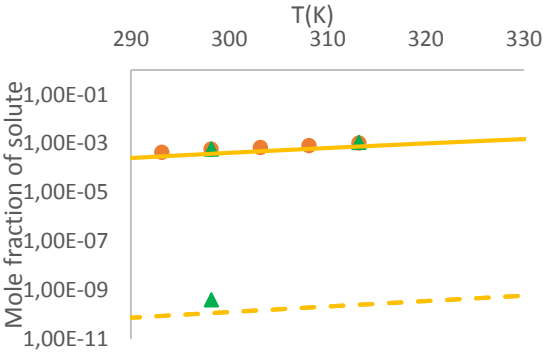

Figure 7- Mole fraction of water in n-undecane (solid line) and of n-undecane in water (dotted line) as a function of temperature; experimental data from (Maczynski A. , Shaw, Goral, & Wisniewska-Goclowska, 2005)(triangles); experimental data from (Morgado, 2011) (circles); SAFT- γ-Mie results (yellow line).

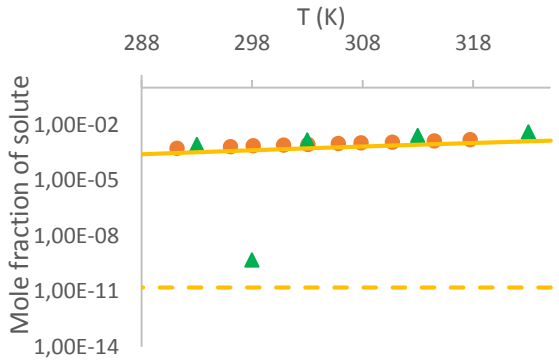

Figure 8- Mole fraction of water in n-hexadecane (solid line) and of n-hexadecane in water (dotted line) as a function of temperature; experimental data from (Maczynski A. , Shaw, Goral, & Wisniewska-Goclowska, 2005)(triangles); experimental data from (Morgado, 2011) (circles); SAFT- γ-Mie results (yellow line).

As can be observed for all systems, the SAFT-γ-Mie solubility line follows thoroughly the solubility data in the oil rich phase. The water rich phase predictions aren't as accurate as the oil-rich phase, showing differences of one order of magnitude. However, this can be considered a relatively good prediction, taking into account that the absolute solubility values on this phase are extremely low.

Table 3- Group parameters within the SAFT-γ Mie GC approach used in the present work (Dufal, Papaioannou, Sadeqzadeh, & Pogiatzis, 2014).

Group	vk*	S_k	λ^r_{kk}	λ^a_{kk}	σ_{kk} [Å]	(ϵ_{kk}/k_B) (K)
H2O	1	1,0000	17,0504	6	3,01	266,684
CH3	1	0,5726	15,0498	6	4,08	256,766
CH2	1	0,2293	19,8711	6	4,88	473,389

Table 4- ϵ_{kl}, estimated from experimental data, and λ^r_{kl}, obtained from equation 18, used within the SAFT-γ Mie approach. In all cases the σ_{kl},d d_{kl} and $\lambda_{kl}{}^a$ are obtained from Equations 16, 17, and 18, respectively (Dufal, Papaioannou, Sadeqzadeh, & Pogiatzis, 2014).

Group k	Group l	ϵ_{kl}/kB (K)	λ^r_{lk}
CH3	H2O	274,80	16,01
CH2	H2O	284,53	18,39
CH2	CH3	350,77	17,26

Table 5- $\epsilon^{HB}{}_{kl,ab}$ and $K_{kl,ab}$ parameters used within the SAFT-γ Mie approach. (Dufal, Papaioannou, Sadeqzadeh, & Pogiatzis, 2014)

Group k	Site a of group k	Group l	Site b of group l	ϵ_{kk}/k_B (K)	$K_{kl,ab}$[° A³]
H20	H	H20	e1	1985,4	101,7

Thermodynamic Functions

The main standard thermodynamic functions of solution can be calculated from the temperature dependence of the experimental solubility data. For that purpose, the previously presented solubility results were used to obtain the standard enthalpy of solution, $\Delta_{sol}H^0_m$, and the standard entropy of solution, $\Delta_{sol}S^0_m$.

The apparent standard molar Gibbs energy of solution at constant pressure for an ideal mixture is given by the following equation.

$$\Delta_{\mathrm{sol}}\mathrm{G}^0_{\mathrm{m}}(\mathrm{P},\mathrm{T},\mathrm{x}_{\mathrm{i}}) = -\mathrm{RT}\ln \mathrm{x}_{\mathrm{i}} \qquad (21)$$

Assuming that the $\Delta_{sol}H^0_m$ and $\Delta_{sol}S^0_m$ are temperature independent and that the dissolution process takes place at constant temperature and pressure, the following relation is valid,

$$\Delta_{sol}G^0_m(P,T,x_i) = \Delta_{sol}H^0_m - T\Delta_{sol}S^0_m \qquad (22)$$

Relating equations 21 and 22 one can use the following equation to obtain $\Delta_{sol}H^0_m$ and $\Delta_{sol}S^0_m$, from the temperature dependence of the solubility ($\Delta_{sol}H^0_m$ is the slope and the $\Delta_{sol}S^0_m$ is the intercept)

$$\ln \mathrm{x}_1 = -\frac{\Delta_{\mathrm{sol}}\mathrm{H}^0_{\mathrm{m}}}{\mathrm{RT}} + \frac{\Delta_{\mathrm{sol}}\mathrm{S}^0_{\mathrm{m}}}{\mathrm{R}} \qquad (23)$$

For real solutions equation 21 should be expressed in terms of the activity coefficient of the solute, γ_i.However, for very dilute solutions it is known that the change of γ_i with composition becomes negligible. Thus, equation 23 can be used to calculate $\Delta_{sol}H^0_m$ and $\Delta_{sol}S^0_m$.

It is useful to consider the solvation process, in which the energies associated with extracting the solute molecules from the liquid solute are

not considered. To obtain the standard molar enthalpy of solvation, $\Delta_{svt}H_m^0$, one can just subtract the molar enthalpy of vaporization of the solute, $\Delta_l^g H_m^0$, from the standard enthalpy of solution, $\Delta_{sol}H_m^0$. Similarly, the standard molar entropy of solvation, $\Delta_{svt}S_m^0$ was obtained subtracting the molar entropy of vaporization, $\Delta_l^g S_m^0$ from the standard entropy of solution, $\Delta_{sol}S_m^0$.

SAFT-VR-SW with an average k_{ij}

In order to grasp the variation of the thermodynamic properties with the chain length of the n-alkane chemical family, a different strategy was used. The SAFT-VR-SW equation was used to obtain theoretical predictions for a series of water/n-alkane binary systems, using a single average binary interaction parameter was used, k_{ij}=0,29. For the sake of consistency, the pure component's parameters were obtained from correlations with the molar weight, equations (Paricaud, Jackson, & Galindo, 2004).

Results and discussion

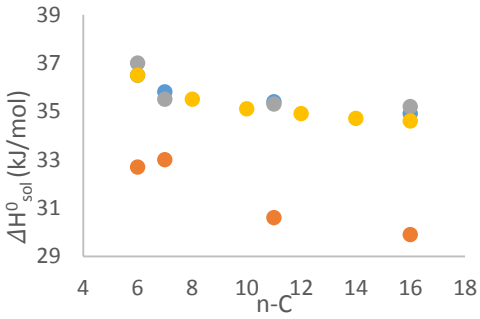

Figure 9- Variation of the ΔH^0_{sol} (kJ/mol) with the carbon number of the n-alkane. Calculated ΔH^0_{sol} (kJ/mol) obtained with: SAFT- γ –Mie (grey dots); SAFT-VR-SW with the k_{ij} value adjusted to the oil rich phase (blue dots); SAFT-VR-SW with an average k_{ij} (yellow dots); Experimental results from (Morgado, 2011) (orange dots).

From figure 11 it is clear that, as a whole, the experimental values (orange) evidence a more acute decrease of the $\Delta_{sol}H^0$ with the n-alkane chain length. The different theoretical predictions are very similar and able to reproduce the experimental trend although with an absolute difference of about 4-5 kJ.mol^{-1}.

Although the nature of all analyzed systems is very similar (water/n-alkane mixtures), the mixtures were studied within the same temperature range, thus at different reduced temperatures rages, therefore at different thermodynamic states. In figure 12 the enthalpy of solvation for all systems was plotted as a function of the average reduced temperature.

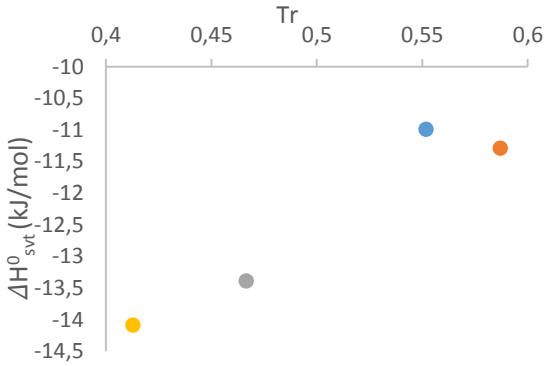

Figure 10- Standard enthalpy of solvation, H^0_{svt}, for each binary system at its reduced temperature. Water/n-hexadecane (yellow), water/n-undecane (grey), water/n-heptane (blue), water/n-hexane (orange).

One can observe that although the $\Delta_{svt}H^0$ is larger (more negative) for the water/n-hexadecane mixture, its reduced temperature is also the lowest and hence the solvent is denser. Figure 12 thus shows that the decrease of $\Delta_{svt}H^0$, is a result not only of the increase of the chain length of the alkane but also of the decrease of the reduced temperature of the solvent.

Conclusions

It was found that the binary interaction parameter, k_{ij}, of the SAFT-VR-SW theory, can be adjusted to reproduce very accurately the oil rich phase of water/n-alkane mixtures from n-hexane to n-hexadecane, and the optimal value to reproduce these systems is very similar and within the rage of 0,30 to 0,28. It was also found that fitting the k_{ij} to the oil rich phase lowers the solubility on both phases, allowing for a better description of the oil rich phase but underpredicting the water rich phase solubility curve.

SAFT- γ –Mie theory was proven to present the best prediction of the solubility of water/n-alkane systems, with both phases accurately reproduced. Another important conclusion that

can be established is that the model can reproduce more accurately the oil rich phase than the water rich phase.

The results also show that the thermodynamic decrease with the chain length of the alkane. The decrease predicted by the theory is less pronounced than that found experimentally and deviates from the experimental values by 5 $J.mol^{-1}$. The predictions of all theoretical treatments are very equivalent.

Bibliography

Blas, F. J., & Vega, L. F. (1997). *Mol. Phys.* , 35.

Chapman, W. G., Gubbins, K. E., Jackson, J., & Radosz, M. (1989). *Fluid Phase Equilibria 52*.

Clark, G. N., Haslam, A., Galindo, A., & Jackson, G. (2006). Developing optimal Wertheim-like models of water for use in Statistical Associating Fluid Theory (SAFT) and related approaches. *Molecular Physics, Vol. 104*.

Dufal, S., Papaioannou, V., Sadeqzadeh, M., & Pogiatzis, T. (2014). Prediction of thermodynamic properties and phase behaviour of fluids and mixtures with the SAFT-γ Mie group contribution equation of state.

Ferguson, A. L., Debenedetti, P. G., & Panagiotopoulos, A. Z. (2009). Solubility and Molecular Conformations of n-Alkane Chains in Water. *Journal of Physical Chemistry*.

Galindo, A., & Mccabe, C. (2010). SAFT Associating Fluids and Fluid mixtures (Chap 8). In A. R. Goodwin, J. Sengers, & C. J. Peters, *Applied Thermodynamics of Fluids* (pp. 215-279).

Gil-Villegas, A., Galindo, A., Whitehead, P. J., Mills, S., Jackson, G., & Burgess, A. N. (1997). Statistical associating fluid theory for chain molecules with attractive potentials of variable range. *The Journal of Chemical Physics*, pp. 106, 4168–4186.

Gross, J., & Sadowski, G. (2001). *Ind. Eng. Chem. Res.*, 1244-1260.

Maczynski, A., Shaw, D. G., Goral, M., & Wisniewska-Goclowska. (2005). IUPAC-NIST Solubility Data Series. 81. Hydrocarbons with Water and SeawaterPart 4. C 6 H 14 Hydrocarbons with Water. *Journal of Physical and Chemical*.

McCabe, C., Galindo, A., Gil-Villegas, A., & Jackson, G. (1998). Predicting the High-Pressure Phase Equilibria of Binary Mixtures of Perfluoro-n-alkanes +n-Alkanes Using the SAFT-VR Approach. *Journal of Physical Chemistry* .

Morgado, P. (2011). *Semifluorinated Alkanes – Structure – Properties Relations,PhD Thesis Pag 153-156.* Lisboa: IST Lisboa.

Papaioannou, V., Lafitte, T., Avendaño, C., Adjiman, C. S., Jackson, G., Müller, E. A., & Galindo, A. (2014). Group contribution methodology based on the statistical associating fluid theory for heteronuclear molecules formed from Mie segments. *The Journal of Chemical Physics*.

Paricaud, P., Jackson, G., & Galindo, A. (2004). Modeling the Cloud Curves and the Solubility of Gases in Amorphous and Semicrystalline Polyethylene with the SAFT-VR and Approach and Flory Theory of Crystallization. *Ind. Eng. Chem. Res. Vol.43, No. 21*, pp. 6871-6889.

Patel, B., Galindo, A., & Maitland, G. (2003). Prediction of the Salting-Out Effect of Strong Electrolytes on Water + Alkane Solutions. *Ind. Eng. Chem. Res.* , 3-5.

Vega, L. F., Llovell, F., & Blas, F. J. (2009). Capturing the Solubility Minima of n-Alkanes in Water by Soft-SAFT. *J. Phys. Chem.* , 7621–7630.

Wisniewska-Goclowska, B., Shaw, D., Skrzecz, A., Góral, M., & Maczynski, A. (2003). Mutual Solubilities of Water and Alkanes. *Monatshefte fur Chemie*.